Doctoral School on Engineering Sciences
Università Politecnica delle Marche

Extended summary

A low-cost structural health monitoring system for residential buildings: experimental tests on a scale model.

Curriculum: Architettura, Costruzioni e Strutture

Author

Daniela Isidori

Tutor(s)

Stefano Lenci

Cristalli Cristina

Date: 30-01-2013

Abstract. One of the most important issues in civil and in mechanical engineering is the detection of structural damages. Throughout its service life, a civil structure besides the exposure to operational and environmental forces can be subjected episodically to earthquakes. These events may have a deep impact on building safety and a continuous monitoring of the structure health conditions becomes desirable or necessary in many cases. Structural Health Monitoring (SHM) provides a valuable knowledge of the dynamic behaviour of monitored structures. Referring to earthquake damage assessment, SHM is spreading from big infrastructures like bridges, dams and skyscrapers to historical heritage and public or residential buildings. Within this a background, the purpose of this work is to propose a new combined experimental and numerical methodology to perform the SHM of civil structures lying in seismic hazard zones. A relatively low-cost SHM prototype system based on this approach has been developed and the issues related to the usage of low-cost sensors and new generation data acquisition tools for non-destructive structural testing are discussed. Moreover, the usage of low-cost sensors has allowed to get enough comparable performance, in terms of measured quantities, with respect to piezoelectric accelerometers. The data acquired by the system are provided to a finite element numerical model (FEM) to detect the appearing, rise and distribution of local damages and to estimate a global damage level. The system has been tested and calibrated on a three-story scale model. Dynamic

tests have been carried out by using two different types of sensors in order to make a comparative analysis of floor noise, dynamic response and phase shift in different operating conditions: (i) low cost MEMS-based accelerometers and (ii) classical piezo-electric transducers. The damage level estimation procedure has been calibrated by comparing the experimental quantities measured during cyclic failure tests of the scale frame, with the FEM model prediction, expressed in terms of cumulated plasticity, obtained by performing non-linear static and dynamic forced response analyses in the time domain. The results obtained show that the numerical model damage state calculation and failure pre-diction are reliable, at least with regards to the experimental tests performed on the scale model.

Keywords. Structural Health Monitoring (SHM), Dynamic analysis, Damage index, Plastic accumulation, Fatigue life.

1 Introduction

One of the most important issues in civil and mechanical engineering is the detection of structural damages (Figure 1).

Figure 1. Example of damage to a building due to the Emilia earthquake in 2012.

Throughout its service life, a civil structure can be subjected to random seismic loading. Structural damage caused by earthquakes may be due to excessive deformation of the elements, or may occur as a result of damage accumulation. The accumulated damage could jeopardize the structural serviceability by even leading to a decreased structural safety. A control of health condition of the structure becomes desirable and necessary for building safety.

The development of low cost and low energy measuring devices, the new generation of acquisition systems, and the increasing availability of software for advanced computational analysis, make possible the extension of SHM from big infrastructures like bridges, dams and skyscrapers [1] to historical heritage and public or residential buildings.

Within this background, the aim of this research is to propose a novel combined experimental and numerical methodology to perform the SHM of civil structures lying in seismic hazard zones. A low cost SHM prototypic system based on this approach has been developed. This monitoring system methodology concerns two different strategies: a periodic long term data acquisition, intended to reveal changes of long term evolution of structural features and performance in order to update the evolution of numerical model parameters and to detect damage due to ageing; and occasionally analyses, aimed at estimating the state of health of a structure at a particular time or after a special event (e.g. strong overloading, earthquakes). For this type of data acquisition a threshold is fixed: if the dynamic input amplitude exceeds this value the system starts to store data and to transfer them to numerical model for damage evaluation. In ordinary conditions, the data continuously collected are periodically deleted.

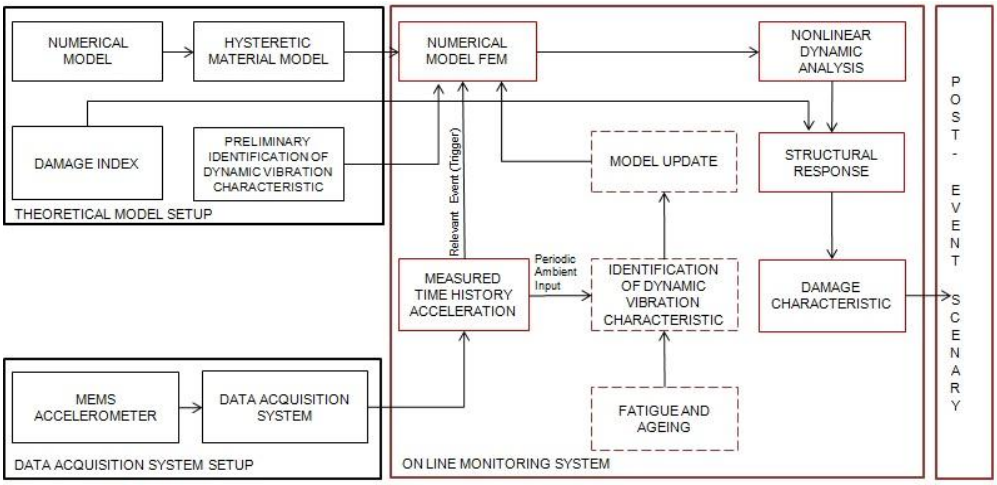

Figure 2. Flow chart of SHM system.

This methodology requires a preliminary work on the diagnostic system and on the theoretical model (Figure 2). The first one includes the Data Acquisition system setup and the calibration of the accelerometer devices. The theoretical model setup, instead, provides the tuning of a finite element (FE) model by means of the preliminary identification of dynamic vibration characteristic, the study of hysteretic material model and the analysis of damage characteristics.
Moreover, one of the goals of this study is to establish a damage model that can be implemented within this monitoring system. The damage analysis requires the study of experimental behaviour of the structure subjected to cyclic loads [2][3][4].
For this reason a three stories aluminium scale model has been built, placed on a slip table and tested with different accelerometers applied to each floor and connected to a data acquisition system in order to detect the collapse capacities of structures under cyclic load [5][6].

2 The experimental set-up

The scale model is a one span aluminium frame with three stories and different heights. The distances between the centroid of the pillars are 246.5 mm along *x*-direction and 107 mm along *y*-direction. Different geometrical configurations have been tested in order to make a comparative study of different structural dynamic behaviour. The typologies examined comprise symmetrical and non-symmetrical structures with different story height level or different floor stiffness. For example, one of the scale model tested has a non-symmetric configuration with different heights (252 mm for the first floor and 172 mm for the second and the third floors). In order to increase the vulnerability of the structure, a bar has been rotated in the second and third level to raise the floor stiffness of these levels. In this way typical *soft-story* behaviour is amplified in the first level. The bars have a rectangular cross section (5 x 10mm) and are made of a standard aluminium alloy AlMgSi 6060 with a T6 heat treatment.
The frame is placed on a slip table with one degree of freedom in the *x*-direction. The model is shown in Figure 3.

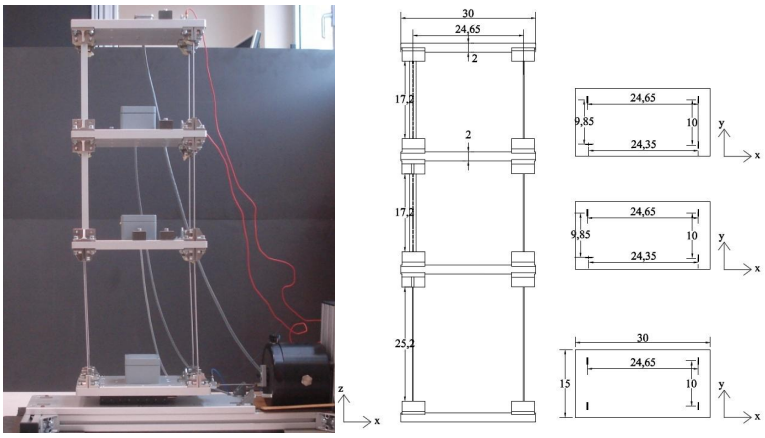

Figure 3: Left: Scale model. Right: Working drawing.

2.1 Accelerometer devices and Data Acquisition System

The data acquisition instrumentation and inter-connections between the equipment are as follows: an electrodynamic vibrator (B&K Type 4809); a piezoelectric load cell (PCB 208C01) placed between the model base and the shaker stinger to measure force at the driving point; 4 piezoelectric IEPE 100 mV/g accelerometers fastened to each floor, starting from ground to top: ACC.#0 PCB 353, ACC. #1 B66B&K 4514-001, ACC #2 Endevco A56-100, ACC #3 PCB 353; and 2 kind of sensors based on MEMS accelerometers: a breakout board made with a Freescale Semiconductor MMA7361L 1.5g 3-axis (placed on 3rd floor) and a ST Microelectronics LIS2L02AS4 2-axis 2g linear accelerometer (the chip has been integrated in custom electronic circuit for power supply regulation, output voltage filtering and impedance adaptation made by AEA srl – Loccioni Group). Each one has been calibrated before the experiment on a B&K 4294 exciter [7][8][9].

3 Experimental identification of the structure

The identification of the dynamic behaviour of the studied structure plays a fundamental role in the proposed approach, since modal parameters are used to tune the numerical model.

In the field of vibration-based experimental structural identification, Experimental or Input-Output Modal Analysis (EMA) and Operational or Output-only Modal Analysis (OMA) test activities can be performed. Both those techniques lead to the evaluation of the so-called modal parameters (natural frequencies, damping factors, mode shapes) and, hence, to the complete characterization of the dynamic behaviour of the system under test.

In the case of large civil or mechanical structures, an EMA implementation could become complicated by the fact that exciting the structure could not be simple. Moreover, the environmental excitation would provide the system with an external not known input that, in

the EMA case, would lead to the estimation of not correct FRFs. In the OMA case, instead, the environmental unknown excitation generally satisfies the recalled main assumption, since peaks are usually not present in the spectra that could lead to extra-peaks in the output responses, not related to structural modes. OMA becomes, indeed, the suitable approach in those situations and, moreover, a really interesting tool to perform continuous vibration-based SHM.
In this section the structural identification of the scale model depicted Figure 3 is performed by using the OMA approach. The operational modal identification technique utilised for the cross power spectral densities (CPS) post-processing and modal parameter estimation has been the Polyreference Least Square Complex Frequency Domain modal estimation techniques, also known as the PolyMAX algorithm [10][11][12]. The results obtained in terms of eigenfrequencies and damping ratios are represented in Table 1.

Table 1: OMA natural frequencies and damping ratios

Mode	natural frequency [Hz]	damping ratio [%]
Mode 1	0.9129 Hz	1.69 %
Mode 2	5.445 Hz	2.69 %
Mode 3	12.54 Hz	0.413 %
Mode 4	19.37 Hz	0.487 %
Mode 5	30.45 Hz	0.904 %
Mode 6	34.96 Hz	0.125 %

The first, the fourth and the seventh natural frequencies correspond to modes mainly belonging to the xz-plane. The second and the sixth natural frequencies represent the first and the second eigenvalues in the y-direction while the third and the fifth correspond to torsional modes. In Figure 4 some of the obtained mode shapes are represented.

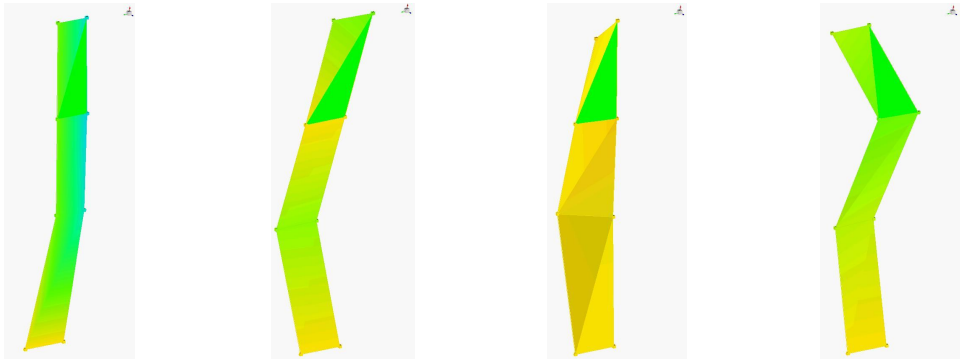

mode 1 (0.9129 Hz, 1.69 %) | mode 4 (19.37 Hz, 0.487 %) | mode 6 (30.45 Hz, 0.904 %) | mode 7 (34.96 Hz, 0.125 %)

Figure 4: Representation of some of the obtained OMA modes

4 P - Δ effects on static and dynamic responses

In flexible structures if gravity loads are high in proportion to the lateral stiffness the contributions of secondary effects are highly amplified and can change the displacements and member forces, the dynamic characteristics, and thus may be a source of sideway collapse. However, in Civil Structural Engineering it is commonly referred to as P-Δ geometrical effect.

The evaluation of structural vulnerability due to P- Δ effect can be obtained through a pushover analysis. During this non-linear static analysis, the structure is subjected to lateral load patterns proportional to the first mode and incremented on each step.

The capacity curve plotting, in particular, the base shear against the upper floor *x*-displacement is shown in Figure 5, both with and without this second order effect for lumped and distributed plasticity models.

The P- Δ effect on the pushover curve demonstrates (i) the initial reduction of the elastic stiffness and (ii) a somehow expected softening behaviour, i.e. a negative stiffness in the plastic range of deformation [13].

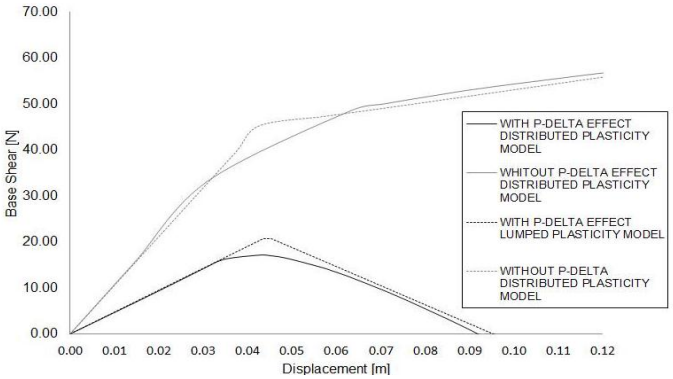

Figure 5: Global capacity pushover curves of the structure obtained with lumped and distributed plasticity model.

Therefore, the considered structure becomes vulnerable to collapse induced P-Δ effect when it reaches a state of instability with zero static lateral resistance. This happens when the displacement of the upper floors (equivalent to that of the first floor in the case of the scale model) is $\Delta^{lim} = 0.092$m (see Figure 5).

Since the P-Δ effect can change the displacements and member forces, and then the dynamic characteristics, it has to consider this effect also in the linear dynamic analysis of the numerical model in order to obtain the effective tangent stiffness and the relative natural frequencies comparable with those obtained experimentally [14].

In Table 2 is represented the comparison of theoretical and experimental natural frequencies. Only the first natural frequency is clearly affected by the P-Δ geometric effect. Due to the higher story stiffness of the upper floors the associated modal shape (see Figure 4 and Figure 6) is basically a rigid body motion of the floors over the low level pillars, thus all the masses are subjected to extensive shifting. This instead does not occur for higher modes.

Table 2: Experimental frequencies versus numerical results

Mode	OMA Natural Frequencies [Hz]	Numerical Natural Frequencies without P-Δ effect [Hz]	Numerical Natural Frequencies with P-Δ effect [Hz]
Mode 1	0.9129	1.349	0.9164
Mode 2	5.445	8.653	8.565
Mode 3	12.54	10.35	10.32
Mode 4	19.37	19.43	19.33
Mode 5	27.57	27.27	27.04
Mode 6	30.45	32.53	32.47
Mode 7	34.96	34.17	34.04

Therefore the reference frequencies are those obtained with second order effect.
The mode shapes relative to the three frequencies obtained are plotted in Figure 6.

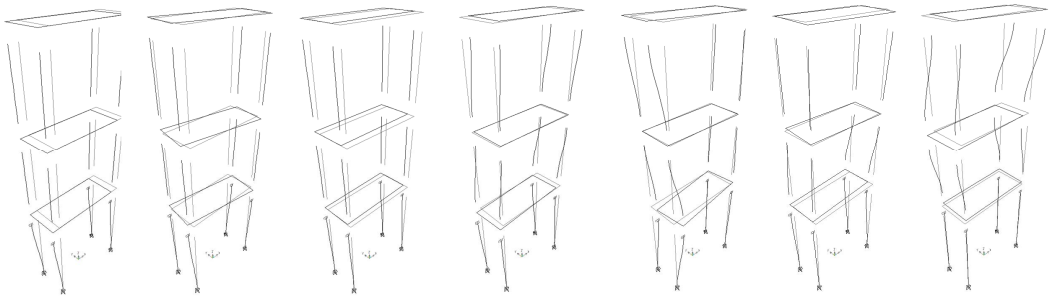

Figure 6: Representation of the modal shapes obtained with numerical model

As shown in Table 2 and in Figure 6, the natural frequencies and the modal shapes experimentally identified match the ones numerically calculated by the model.

5 Damage Index

The primary objective of this monitoring system is to generate a post-event scenario by providing additional support for decision-making in emergency management. The tuning of reliable local and global damage indexes is a significant result for the evaluation of post-event structural integrity of buildings.
Collapse may be local or global, and different damage indexes are adopted to describe global and local collapse of this particular configuration.
In this case, the model is a flexible ductile structures so gravity loads acting through lateral displacements amplify structural deformations and stress resultants, and thus may be a source of sideways collapse. In fact, global collapse may imply dynamic instability, usually triggered by large story drifts, which are amplified by P- Δ effects and deterioration in strength and stiffness of the system components [15].

5.1 Fatigue Damage Index

One of the basic aspects when studying cycling loads effects on this ductile flexible model is predicting the fatigue life of the structure subjected to a stress-strain time history. Complete information about the behaviour of the material subjected to cyclic loading is necessary to make this prediction, in addition to the characterization of the cyclic stress-strain response.
In this study, failure due to fatigue occurs after a number of cycles in the order of 10^3. For this reason, it is more appropriate referred to low-cycle fatigue [16]. Low fatigue cycle is based on the analysis of strain life because the account in terms of stress (usually considered in the prediction of high cycle fatigue life) is not as useful and material strain offers a simpler description.
There are two strain components that characterize the cyclic stress-strain curve: the linear-elastic portion (ε_E) and the plastic stress-strain (ε_p). The total strain-life equation is made up of an elastic and plastic term. This relation is usually characterized by the strain-life equation [17]

$$\frac{\Delta\varepsilon}{2} = \frac{\Delta\varepsilon_E}{2} + \frac{\Delta\varepsilon_P}{2} = \frac{\sigma_f'}{E}(2N)^b + \varepsilon_f'(2N)^c \qquad (1)$$

where $\Delta\varepsilon/2$ is the total strain amplitude, σ'_f the fatigue strength coefficient, ε_f' is an empirical constant known as the fatigue ductility coefficient, $2N$ is the number of reversals to failure (N cycles), c and b are empirical constants known as respectively the fatigue ductility exponent and strength ductility exponent.
The fatigue ductility and strength properties of the 6060 – T6 alloy are obtained experimentally and are reported in Table 3 [17].

Table 3. Cyclic stress–strain curve parameters for Aluminium alloy 6060 – T6

Fatigue strength coefficient, σ'_f[MPa]	376.5
Fatigue strength exponent, b	-0.084
Fatigue ductility exponent, c	-0.537
Fatigue ductility coefficient, ε'_f	0.157

Fatigue life can be influenced by several factors: mean stress, load sequence, geometry (notches and variation in cross-section), surface quality, etc. These improvements are normally observed especially in high-cycle fatigue but, in any case, they could also affect low-cycle fatigue life. For these reasons in this work two different corrections of the Equation 1 that include the effects of mean stress are considered: *Morrow*'s [17] and *Manson and Halford*'s [18] correction.
A common application of the strain-life approach involves fatigue analysis of notched members, because the deformation of the material at the notch root is often inelastic, and notch stresses and strains are explicitly considered in the strain-life approach, whereas the ε-N curves approach only concerns nominal stresses.
Fatigue fractures can be initiated by these notches. The degree of stress and strain concentration is a fundamental factor in estimating the fatigue strength of notched parts.
Neuber's rule is the most widely used notch stress-strain model. It is expressed as [20]

$$k_\varepsilon k_\sigma = \frac{\varepsilon_{eff}}{\varepsilon_{nom}} \frac{\sigma_{eff}}{\sigma_{nom}} = k_t^2 \tag{2}$$

where k_ε k_σ are the strain and stress concentration factor, ε_{eff} or σ_{eff} are the maximum stress or strain at the notch and ε_{nom} or σ_{nom} the nominal stress or strain.
The value K_t is obtained by comparing the numerical response of two numerical FE models: one considers notch effects and allows for obtaining the values of ε_{eff} and σ_{eff}, and the other one without any changes in geometry, allows for obtaining the value of ε_{nom} and σ_{nom}.
By analytically solving the system composed by Equation 2 and the equation of the bilinear stress-strain model we can obtain the value of ε_{eff} and thus the number of reversals before failure from *Morrow*'s and *Manson and Halford*'s correction. Then the fatigue life is evaluated by damage accumulation hypothesis and the total measure of damage (D_f) is calculated with the cumulative *Palmgren - Miner*'s rule [21]. This rule states that the failure occurs when

$$D_f = \sum_{i=1}^{K} \frac{n_i}{N_i} \tag{3}$$

where n_i is the number of applied load cycles of type *i, k* different stress or strain magnitudes, N_i is the pertinent fatigue life obtained from *Morrow*'s and *Manson and Halford*'s correction.

5.2 Ratcheting Damage Index

Since the main purpose of this study is to find an immediate and practical damage detection method, the global damage index due to ratcheting has been considered in this study for its simplicity and immediacy, by directly taking into account the displacement value. In this case, the index is derived from the ratio between inter-story drift Δ^{rel} obtained during the test, the yield displacement Δ^{yield} obtained analytically and ultimate displacement Δ^{lim} calculated with the pushover analysis (see Paragraph 4).

$$D_a = \frac{\Delta^{exp} - \Delta^{yield}}{\Delta^{lim} - \Delta^{yield}} \tag{4}$$

The inter-story drift Δ^{exp} is derived from

$$\Delta^{exp} = \overline{\Delta} + \Delta^{cyc} \tag{5}$$

where $\overline{\Delta}$ is the average displacement of the floor and Δ^{cyc} the relative cyclic displacement between two consecutive floor. This damage index is then activated when displacement reaches the Δ^{yield} value; if $\Delta^{exp} < \Delta^{yield}$, the difference is automatically considered equal to zero.

6 Cyclic failure tests and damage indexes

Different experimental tests obtained from different geometrical configurations (one symmetric with regular height and one with different heights for each floor) are conducted. After a preliminary characterization of material properties, an update of the numerical model and after the experimental determination of the natural frequencies and modes shapes, structural responses are analysed in order to obtain damage quantification. Cyclic

loading tests in the elastic and plastic ranges have been performed in order to verify the reliability of damage indexes previously described. The identification of dynamic characteristics is carried out not only preliminarily for model calibration but also during tests in order to detect the evolution of structural features for model updating. This has been done by temporarily stopping the high amplitude cyclic load and by temporarily applying a low amplitude white noise excitation needed for the modal analysis (done with Transmissibility function or OMA). The high amplitude cyclic loads are sinusoidal inputs where the frequency is close to the first resonant frequency of the scale model (the sinusoidal input has a constant amplitude for each load step). In the cyclic fatigue damage index estimation, white noise inputs intervals are not considered because the input amplitude is negligible.
Three types of damage are singled out: small horizontal surface micro fractures on the lateral skin of the pillars due to bending deformation (*type 1*), the local damage caused by the breaking of at least one of the pillars in one end due to fatigue (*type 2*), and the global collapse for structural instability due to plastic strain accumulation (*type 3*). These different damage levels are gradually reached during different cyclic tests conducted on the different scale frames. Damage *type 2* and *type 3* sometimes are independent: in some cases there is a rupture at the end section of a pillar after the collapse is reached, while in other cases the structural instability is reached without any local crack caused by fatigue damage. Damage *type 1* is not quantified in this study because it represents an overcoming of the elastic limit.

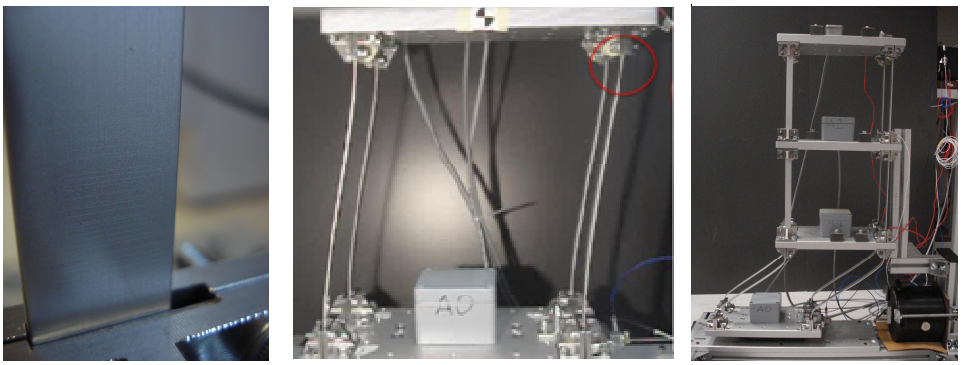

Figure 7: The three types of damage, respectively *type 1*, *type 2* and *type 3*.

The most relevant structural damages are related to two different mechanisms and consequently, two separate indexes, previously described, are considered: the pure cyclic fatigue damage index D_f, and the ratcheting index D_a. The former measures the damage due to degrading or ageing, whereas the latter accounts for the damage due to a significantly dangerous event.
The maximum level that each of the two damage indexes can individually achieve (i.e. 100 %) corresponds (i) to the state of fatigue failure of at least one of the structural components *type 2* (for D_f), and (ii) to the collapse of the structure due to bending instability *type 3*
(for D_a).
Different damage scenarios are studied in this thesis (they are described in a scientific paper that will soon be submitted) and the monitoring campaign shows all the type of damage previously described.

The damage indexes and then the life prediction of the scale model obtained with the different cyclic failure tests are reliable with experimental results.

7 Conclusion

In this work a new combined experimental and numerical methodology to perform the SHM of civil structures lying in seismic hazard zones is proposed. A low cost SHM prototype system based on this approach has been developed. This monitoring system methodology concerns two different strategies: a periodic long term data acquisition, intended to reveal changes of long term evolution of structural features and performance in order to update the evolution of numerical model parameters and to detect damage due to ageing; an occasionally surveys, aimed at estimating the state of health of a structure at a particular time, subsequent to some special event (e.g. earthquakes). This methodology required a preliminary setting of the diagnostic system and of the theoretical model.
A scale frame model of a three-story building has been build up and instrumented in order to simulate the vibration response of a multi-story building subjected to cyclic loads.
The damage detection procedure adopted is characterized by the following steps:
- Identification of modal parameters for the tuning of the numerical model with the transmissibility function or OMA analysis;
- Non-linear static analysis in order to obtain the monotonic behaviour of structure with the P-Δ effect;
- Experimental test in elastic-plastic range in order to obtain damage applying a sinusoidal input at the base of the scale model;
- Damage level evaluation using local and global damage index.
The structural damage is related to two different mechanisms and consequently two separate indexes are introduced: the pure cyclic fatigue damage index, referred to as D_f, and the ratcheting one, D_a. The former measures the damage due to degrading or ageing, whereas the latter accounts for the damage due to a significantly dangerous event.
Cyclic loading tests in the elastic-plastic range are performed to detect indexes of local and global damage mechanisms and to test the devices, the system architecture studying the dynamic characteristics of the structure, and the reliability of the numerical model compared with experimental results.
A damage level estimation methodology is proposed and calibrated comparing the experimental results with the model prediction during cyclic failure tests of the scale frame.
The life prediction of the scale model obtained by damage indexes, estimated from the measurement acquired with a low cost SHM system is consistent with experimental results.

References

[1] Ragland, W. S., D.Penumadu & Williams, R. T. *Finite element modeling of a full-scale five-girder bridge for structural health monitoring*. Structural Health Monitoring, vol.10, pp.449-465, 2011.
[2] Araki, Y., Hjelmstad, K. D. *Criteria for assessing dynamic collapse of elastoplastic structural systems*. Earthquake Engineering & Structural Dynamics, vol. 29, pp.1177-1198, 2000.
[3] Colombo, A., Negro, P. *A damage index of generalized applicability*. Engineering Structures, vol. 27, pp.1164-1174, 2005.
[4] Cosenza, E., Manfredi, G. *Indici e misure di danno nella progettazione sismica*. CNR-Gruppo Nazionale per la Difesa dai Terremoti, vol. 125, 2000.

[5] Miranda, E. Asce, M. & Akkar, S. D. *Dynamic Instability of Simple Structural Systems*. Journal of Structural Engineering, vol.129, pp.1722-1726, 2003.

[6] Duyi, Y., Zhenlin, W. *A new approach to low-cycle fatigue damage based on exhaustion of static toughness and dissipation of cyclic plastic strain energy during fatigue*. International Journal of Fatigue, vol.23, pp.679-687, 2001.

[7] Adams, P. *Using Micro-ElectroMechanical Systems (MEMS) accelerometers for earthquake monitoring*. Australian Earthquake Engineering Society Member Articles, June 2009.

[8] Albarbar, A., Mekid, S., Starr, A., Pietruszkiewicz, R., *Suitability of MEMS Accelerometers for Condition Monitoring: An experimental study*. Sensors, vol.8, pp.784-799, 2008.

[9] Isidori, D., Concettoni, E., Cristalli, C., Lenci, S. *Experimental Setup for Real Time Structural Health Monitoring: Data Acquisition and Structural Modelling Issues*. Proceedings of ICEDyn 2011, Tavira (PT), ISBN: 978-989-96276-1-1, 2011.

[10] Peeters, B., Van der Auweraer, H., Guillaume, P. and Leuridan, J., *The PolyMAX frequency-domain method: A new standard for modal parameter estimation?* Shock and Vibration, vol.11, pp. pp.395−409, 2004.

[11] Van der Auweraer, H., Guillaume, P., Verboven, P. and Vanlanduit, S., *Application of a fast-stabilizing frequency domain parameter estimation method*. ASME Journal of Dynamic Systems, Measurement, and Control, vol.123, pp. 651–658, 2001.

[12] Heylen, W., Lammens, S. and Sas, P., *Modal Analysis Theory and Testing*. K.U.Leuven, Belgium, 2007.

[13] Bernal D., *Instability of buildings during seismic response*. Engineering Structures, vol.20, pp. 496-502, 1998.

[14] Wilson, L. E. *Three dimensional static and dynamic analyses of structures: a physical approach with emphasis on earthquake engineering*. Computer & Structures, I. (Eds.), 1998.

[15] Asimakopoulos, A. V.; Karabalis, D. L. & Beskos, D. E. *Inclusion of P-Δ effect in displacement-based seismic design of steel moment resisting frames*. Earthquake Engineering & Structural Dynamics, vol.36, pp.2171-2188, 2007.

[16] Yao, J., Munse, W. *Low-cycle fatigue of metals. Literature review*. Ship Structure Committee Washington DC, 1961

[17] Borrego, L.P., Abreu, L. M., Costa, J.M., Ferreira, J.M. *Analysis of low cycle fatigue in AiMgSi Aluminium alloys*. Anales de Mecanica de la Fractura. vol.20, pp. 179-184, 2003

[18] Manson, S. & Halford, G. *Practical implementation of the double linear damage rule and damage curve approach for treating cumulative fatigue damage*. International Journal of Fracture, vol.17, pp.169-192, 1981.

[19] Fatemi, A., Zeng, Z. *Elasto-plastic stress and strain behaviour at notch roots under monotonic and cyclic loadings*. Journal of strain analysis, vol. 36, pp.287-300, 2001.

[20] Fatemi, A. & Zeng, Z. *Elasto-plastic stress and strain behaviour at notch roots under monotonic and cyclic loadings*. Journal of strain analysis, vol. 36, pp.287-300, 2001.

[21] Adam, C., Ibarra L., *Cumulative fatigue damage and life prediction theories: a survey of the state of the art for homogeneous materials*. International Journal of Fatigue, vol.20 (1), pp. 9-34, 1998.